https://doi.org/10.5194/amt-2019-174
Preprint. Discussion started: 25 June 2019

Atmospheric Measurement Techniques Discussions

A Comparative Evaluation of Aura-OMI and SKYNET Near-UV Single-scattering Albedo Products

Hiren Jethva[1,2*], Omar Torres[2]

[1]Universities Space Research Association, Columbia, MD 21044 USA
[2]NASA Goddard Space Flight Center, Greenbelt, MD 20771 USA

Mailing Address:
Room#A422, Building#33,
Laboratory of Atmospheric Chemistry & Dynamics
Earth Science Division
NASA Goddard Space Flight Center,
Greenbelt, MD 20771, USA

[*]**Corresponding Author: Dr. Hiren Jethva**
E-mail: hiren.t.jethva@nasa.gov

https://doi.org/10.5194/amt-2019-174
Preprint. Discussion started: 25 June 2019

Atmospheric Measurement Techniques Discussions

ABSTRACT

The aerosol single-scattering albedo (SSA) retrieved by the near-UV algorithm applied to the Aura/Ozone Monitoring Instrument (OMI) measurements (OMAERUV) is compared with an independent inversion product derived from the sky radiometer network SKYNET-a ground-based radiation observation network span over Asia and Europe. The present work continues our efforts to evaluate the consistency between the retrieved SSA from satellite and ground sensors. The automated spectral measurements of direct downwelling solar flux and sky radiances made by SKYNET Sun-sky radiometer are used as input to an inversion algorithm that derives spectral aerosol optical depth (AOD) and single-scattering albedo (SSA) in the near-UV to near-IR spectral range. The availability of SKYNET SSA measurements in the ultraviolet region of the spectrum allows, for the first time, a direct comparison with OMI SSA retrievals eliminating the need of extrapolating the satellite retrievals to the visible wavelengths as the case in the evaluation against the Aerosol Robotic Network (AERONET). An analysis of the collocated retrievals from over 25 SKYNET sites reveals that about 61% (84%) of OMI-SKYNET matchups agree within the absolute difference of ±0.03 (±0.05) for carbonaceous aerosols, 50% (72%) for dust aerosols, 45% (75%) for urban-industrial aerosol types. Regionally, the agreement between the two inversion products was robust over several sites in Japan influenced by carbonaceous and urban-industrial aerosols, at the biomass burning site *Phimai* in Thailand, and polluted urban site in *New Delhi*, India. The collocated dataset yields fewer matchups identified as dust aerosols mostly over the site *Dunhuang* with more than half of the matchup points confined to within ±0.03 limits. Combinedly, the OMI-SKYNET retrievals agree mostly within ±0.03 for the AOD (388 or 400 nm) larger than 0.5 and UV Aerosol Index larger than 0.2. The remaining uncertainties in both inversion products can be attributed to specific assumptions made in the retrieval algorithms, i.e., the uncertain calibration constant, assumption of spectral surface albedo and particle shape, and sub-pixel cloud contamination. The assumption of fixed and spectrally neutral surface albedo (0.1) in the SKYNET inversion appears to be unrealistic, leading to a large underestimation of retrieved SSA, especially for low aerosol load conditions. At large AOD values for carbonaceous and dust aerosols, however,

https://doi.org/10.5194/amt-2019-174
Preprint. Discussion started: 25 June 2019

Atmospheric Measurement Techniques Discussions

retrieved SSA values by the two independent inversion methods are generally consistent in spite of the differences in retrieval approaches.

https://doi.org/10.5194/amt-2019-174
Preprint. Discussion started: 25 June 2019

Atmospheric Measurement Techniques Discussions

1 INTRODUCTION

Satellite-based remote sensing of aerosols has become an essential tool to detect, quantify, and routinely monitor the aerosol optical and size properties over the globe. An accurate representation of aerosols in the climate models is an essential requirement for reducing the uncertainty in aerosol-related impact on the Earth's radiation balance (direct and semi-direct effects) and cloud microphysics (indirect effect) (*IPCC*, 2013). The fundamental aerosol parameters determining the strength and sign of the radiative forcing are the aerosol optical depth (AOD) and single-scattering albedo (SSA) in addition to the reflective properties of the underlying surface. While the columnar AOD represents the total extinction (scattering and absorption) resulting from the interactions with solar radiation, SSA describes the relative strength of scattering to the total extinction. Together, both AOD and SSA determine the magnitude and sign of the aerosol radiative forcing. For example, a decrease in SSA from 0.9 to 0.8 can often change the sign of radiative forcing from negative (cooling) to positive (warming) that also depends on the albedo of the underlying surface and the altitude of the aerosols (*Hansen et al*., 1997). Thus, an accurate estimate of both quantities is a prime requirement for reliable estimates of the net effect of atmospheric aerosols produced with the anthropogenic as well as natural activities.

Launched in July 2004, the Ozone Monitoring Instrument (OMI) onboard NASA's Aura satellite has now produced more than a decade long global record of observations of reflected radiation from Earth in the 270–500 nm wavelength range of the spectrum on a daily basis. OMI scans the entire Earth in 14 to 15 orbits with its cross-track swath of ~2600 km at ground level at a nadir ground pixel spatial resolution of 13 × 24 km^2. Satellite observations of the top-of-atmosphere reflected light at 354 and 388 nm wavelengths made by OMI are used to derive the UV aerosol index (UVAI) as well as the AOD and SSA using a near-UV algorithm (OMAERUV) that takes advantage of the well-known sensitivity to the aerosol absorption in the UV spectral region (*Torres et al*., 1998). While a general description of the OMI/OMAERUV algorithm is presented in *Torres et al.* (2007), the recent algorithmic upgrades are documented in *Torres et*

https://doi.org/10.5194/amt-2019-174
Preprint. Discussion started: 25 June 2019

Atmospheric Measurement Techniques Discussions

al. (2013, 2018). The most important changes applied in the latest OMAERUV algorithm upgrade includes: 1) use of new carbonaceous aerosol models that account for the presence of organics in the carbonaceous aerosols by assuming wavelength-dependent imaginary part of the refractive index (*Jethva and Torres*, 2011), 2) an implementation of robust scheme to identify aerosol type (smoke, dust, urban/industrial) that combinedly uses the information on carbon monoxide (CO) observations from the Atmospheric Infrared Sounder (AIRS) and UVAI from OMI (*Torres et al*., 2013), 3) use of the aerosol height climatology dataset derived from the Cloud-Aerosol Lidar with Orthogonal Polarization (CALIOP) lidar-based measurements of the vertical profiles of aerosol for the carbonaceous and dust aerosols (*Torres et al*., 2013), and 4) better treatment of dust particles assuming realistic spheroidal shape distribution (*Torres et al*., 2018). Additionally, the upgraded OMAERUV algorithm has adopted a new method to calculate UVAI, which now accounts for the angular scattering effects of clouds and significantly reduces a scan angle related asymmetry in UVAI over cloudy scenes (*Torres et al*., 2018).

The present work continues our efforts to evaluate the consistency between ground-based SSA measurements and satellite retrievals from near UV observations. On the first attempt to intercompare space-based and surface near UV SSA measurements, Earth Probe TOMS retrievals were compared to AERONET observations acquired during the SAFARI 2000 field campaign (*Torres et al.*, 2005). The OMAERUV near-UV aerosol product of AOD and SSA has been continually assessed and validated against the ground-based measurements acquired from the globally distributed Aerosol Robotic Network-AERONET (*Torres et al*., 2007; *Ahn et al*., 2008; *Jethva and Torres*, 2011; *Ahn et al*., 2014; *Jethva et al*., 2014). While the OMAERUV AOD product was directly validated against the AERONET measurements made in the near-UV (340-380 nm), as carried out in *Ahn et al*. (2014), the SSA retrievals have been evaluated by comparing with an independent ground inversion product of AERONET by *Jethva et al*. (2014). The later analysis required OMI retrievals of SSA to be extrapolated to the shortest visible wavelength of 440 nm of AERONET inversion product to make the comparison possible. Such adjustment in the wavelength of retrievals can introduce uncertainty in the comparison arising

https://doi.org/10.5194/amt-2019-174
Preprint. Discussion started: 25 June 2019

Atmospheric Measurement Techniques Discussions

from inaccuracy of the spectral dependence of absorption assumed in the wavelength conversion.

A direct comparison of the column-integrated SSA at 388 nm retrieved from OMI requires equivalent ground-based columnar retrievals in the near-UV region. The international network of scanning sun-sky radiometers (SKYNET) fulfills this requirement as it performs the direct Sun and sky measurements in the near-UV (340-380 nm) as well as visible/near-IR (400-1020 nm) regions of the spectrum, and derives spectral AOD and SSA at these wavelengths. Taking advantage of the availability of ground-based SSA inversions in the near-UV from SKYNET, we inter-compare the OMI and SKYNET SSA products at several SKYNET sites in Asia and Europe. Since both retrieval approaches are based on inversion algorithms that rely on assumptions, the resulting level of agreement can only be interpreted as a measure of consistency (or lack thereof) in the measurement of the same physical parameter by fundamentally different remote sensing approaches.

The paper is organized as follows: section 2 describes the satellite and ground-based data sets assessed in this analysis along with the collocation methodology; the results of OMI-SKYNET SSA comparison over individual sites, combinedly for each aerosol type, and diagnosis of differences between them are presented in section 3; the possible sources of uncertainty in both inversion products are discussed in section 4; the paper is summarized and concluded in section 5.

2 DATASETS

2.1 THE OMI-OMAERUV AEROSOL PRODUCT

The entire record of OMI observations (October 2004 to present) has been reprocessed recently with the refined OMAERUV algorithm (PGEVersion V1.8.9.1) to derive a comprehensive

https://doi.org/10.5194/amt-2019-174
Preprint. Discussion started: 25 June 2019

Atmospheric Measurement Techniques Discussions

aerosol product that includes the retrievals of UV Aerosol Index (UVAI), AOD, SSA, and AAOD (388 nm) at a pixel resolution of 13 x 24 km^2 at nadir viewing geometry. The retrieved parameters are also reported at 354 nm and 500 nm wavelengths following the spectral dependence of aerosols assumed in the chosen model. The data set is available in the HDF-EOS5 format and can be obtained at no cost from NASA Goddard Earth Sciences (GES)-Data and Information Services Center (DISC) server at http://daac.gsfc.nasa.gov/. The recent upgrade has been documented in detail in the work of *Jethva and Torres* (2011), *Torres et al.* (2013, 2018) and *Ahn et al.* (2014). Here, we use the OMAERUV Level 2 Collection 003 (V1.8.9.1) aerosol product processed in July 2017.

Post-2007, the OMI observations have been affected by a possible external obstruction that perturbs both the measured solar flux and Earth radiance. This obstruction affecting the quality of radiance at all wavelengths for a particular viewing direction is referred to as “row anomaly” (RA) since the viewing geometry is associated with the row numbers on the charge-coupled device detectors. The RA issue was detected first time in mid-2007 with a couple of rows which during the later period of operation expanded to other rows in 2008 and later. At present, about half of the total 60 rows across the track are identified and flagged as row anomaly affected positions for which no physical retrievals are performed (*Schenkeveld et al*., 2017). The details about this issue can be found at http://www.knmi.nl/omi/research/product/rowanomaly-background.php. The RA has significantly affected the sampling during post-2008 OMI measurements, where about half of the OMI swath is blanketed by row anomaly flags. As a result, the availability of the number of retrievals over a particular station is reduced starting in 2009 compared to earlier OMI measurements. Consequently, the OMI-SKYNET matchups are also expected to be lower during the row anomaly affected period. The OMAERUV algorithm assigns quality flags to each pixel which carries information on the quality of the retrieval depending upon the observed condition. We used aerosol retrievals free of RA and flagged as quality flag ‘0’, which are considered best in accuracy due to higher confidence in detecting aerosols in a scene with minimal or no cloud contamination.

https://doi.org/10.5194/amt-2019-174
Preprint. Discussion started: 25 June 2019

Atmospheric Measurement Techniques Discussions

2.2 The SKYNET Aerosol Inversion Product

The SKYNET is an international network of scanning sun-sky radiometers (manufactured by *Prede Co. Ltd.,* Japan) performing routine and long-term measurements of direct and diffuse solar radiations at several wavelengths spanning UV (340 and 380 nm), visible (400, 500, 675 nm), near-IR region (875, 1020 nm), and in shortware-IR (1627 nm and 2200 nm) of the spectrum. The automated measurements of direct and diffuse solar radiations are used to measure spectral AODs and retrieve SSAs and other aerosol optical-microphysical properties (volume size distribution, refractive index, phase function, and asymmetry parameter) at the same standard wavelengths of AOD following an inversion algorithm packaged in the *SKYRAD.pack* software (*Nakajima et al*., 1996; *Hashimoto et al*., 2012). Cloudy observations are screened using the Cloud Screening Sky Radiometer code (*Khatri and Takamura*, 2009).

The SKYNET radiometers come in two flavors, model POM-01 and model POM-02. The POM-01 instrument carries a total of five wavelength filters covering visible to near-IR (400-1020 nm), whereas POM-02 instrument has two additional filters in the UV region (340 and 380 nm) along with the other filters in the visible to shortwave-IR (including 1627 nm and 2200 nm) part of the spectrum. The calibration of each SKYNET radiometer is performed on-site on a monthly basis using the improved Langley method (*Nakajima et al*., 1996, *Campanelli et al*., 2004, 2007). Occasionally, the inter-calibration of radiometers is carried out against the master instrument well-calibrated using the Langley method at a high mountain site, e.g., Mauna Loa. The SKYNET radiometers are also inter-compared with AERONET Cimel Sunphotometers and precision filter radiometers at three observation sites, i.e., *Chiba University* and *Valencia* (*Estelles et al*., 2016), and *Rome* (*Campanelli et al*., 2018) .

Studies in the past have compared AODs (*Estellés et al*., 2012a) and SSAs (*Estellés et al*., 2012b) measured/retrieved from SKYNET and AERONET and shown that AODs are well-correlated and in good agreement, but the SKYNET SSAs are found to be higher than those of AERONET (*Che et al*., 2008; *Hashimoto et al*., 2012). *Khatri et al*. (2016) further pinpoints the factors, such as quality of input data attributed to different calibration and observation protocol, different

https://doi.org/10.5194/amt-2019-174
Preprint. Discussion started: 25 June 2019

Atmospheric Measurement Techniques Discussions

quality assurance criteria, the calibration constant for sky radiances, differences in measured AOD, and surface albedo, responsible for the inconsistent aerosol SSA between AERONET and SKYNET using observations from the four representative sites, i.e., Chiba (Japan), Pune (India), Valencia (Spain), and Seoul (South Korea). More discussion on the sources of uncertainties is presented in section 4.

In this study, we include the SKYNET data acquired over a total of 25 sites distributed mostly across Asia and a few in Europe. The dataset is freely accesible from the data holding portal of the Center for Environmental Remote Sensing (CERes), Chiba University, Japan (http://atmos3.cr.chiba-u.jp/skynet/data.html). Figure 1 shows the geographic distribution of selected sites, whereas Table 1 lists the geo-coordinates of these sites with the associated sensor type (POM-01 or POM-02) and data periods. The SKYNET aerosol product is derived using two different Skyrad packs: version 4.2 and version 5, the differences of which are explained in *Hashimoto et al*. (2012). In this study, we use the SKYNET Level 2 product retrieved using version 5 of Skyrad pack. SKYNET retrievals assigned with cloud flag '0' are included in the analysis, since these measurements are believed to be free of cloud contamination considered as higher quality retrievals. A careful examination of the SKYNET inversion dataset revealed some irregularities in the measurements for many sites, such as irregular patterns in the shape of spectral SSAs, identical values of SSA at near-UV and visible wavelengths, and much larger standard deviation (>0.1) in SSA within a few hours. These spurious measurements were excluded from the present analysis.

2.3 The collocation of OMI and SKYNET Measurements

OMI retrievals correspond to a spatial scale of 13 × 24 km^2 at nadir representing the atmospheric conditions over an area. Unlike the direct measurements of the spectral AOD, which correspond to columnar point measurements, the retrievals made by SKYNET use the sky radiances measured at several discrete angles azimuthally, therefore representing the sky condition observed over a station which is associated with approximately 5 km radius surrounding the Sun photometer site. SKYNET retrieves aerosol optical-microphysical

https://doi.org/10.5194/amt-2019-174
Preprint. Discussion started: 25 June 2019

Atmospheric Measurement Techniques Discussions

properties, including spectral SSA, under all cloud-free conditions and at all aerosol loadings. It is expected that the inversion of retrieved parameters from sky radiances offers better accuracy at larger solar zenith angles owing to the longer optical path and better aerosol absorption signal (*Dubovik et al.*, 2000). These conditions are best satisfied with the measurements made during the early morning and late afternoon hours. On the other hand, Aura/OMI overpasses a station during the afternoon hours with the local equator-crossing time 1:30 P.M. In order to collocate both types of measurements, therefore we select a time window of ±3 h around OMI overpass time in order to get sufficient high-quality SKYNET retrievals particularly from early morning/late afternoon measurements. The OMI retrievals of SSA were spatially averaged in a grid area of 0.5° by 0.5° centered at the SKYNET site. Though the spatial averaging area for the OMI retrieval is about 50 km^2, due to its larger footprint, the actual area intercepted by OMI pixels around SKYNET site is likely to be larger.

OMI performs retrieval at 354 nm and 388 nm wavelengths, whereas the SKYNET POM-02 instrument reports SSA at nearby wavelengths of 340, 380, and 400 nm. To compare both SSA products at the same wavelength, SKYNET SSA was linearly interpolated at 388 nm, to match with the wavelength of OMI retrieval, using the measurements at the two nearest wavelengths, i.e., 380 nm and 400 nm. The SKYNET POM-01 instruments don't carry UV wavelength filters, but report the retrievals at the shortest wavelength 400 nm and other visible/near-IR wavelengths. In this case, the OMI retrievals are extrapolated from 388 nm to 400 nm, to match with the wavelength of SKYNET inversion, following the spectral dependence of SSA associated with the chosen aerosol model in the OMI algorithm.

3 Results

3.1 OMI-SKYNET Comparison over Individual Stations

Figure 2 displays the OMAERUV versus SKYNET SSA scatterplots for selected sites in Japan. The comparison was made at 388 nm or 400 nm depending upon the availability of the SKYNET inversion at those wavelengths, i.e., POM-01 or POM-02 sensors. Legends with different colors

https://doi.org/10.5194/amt-2019-174
Preprint. Discussion started: 25 June 2019

Atmospheric Measurement Techniques Discussions

represent the aerosol type selected by the OMAERUV algorithm for the co-located matchups (N). RMSD is the root-mean-square difference between the two retrievals; Q_0.03 and Q_0.05 are the percent of total matchups (N) that fall within the absolute difference of 0.03 and 0.05, respectively; horizontal and vertical lines for each matchup are the standard deviation of temporally and spatially averaged SKYNET and OMI SSAs. The comparison includes OMI-SKYNET matchups with AOD>0.3 (388 or 400 nm) in both measurements simultaneously. The scatterplots reveal a good level of agreement for matchups identified with carbonaceous aerosols over *Chiba University*, *Cape Hedo*, *Fukue*, *Saga*, and *Etchujima* with the majority of points confined within the absolute difference of 0.03. The OMI-SKYNET dataset are dominated with matchup points identified as the urban/industrial aerosols by the OMAERUV algorithm for which the measured UVAI falls below 0.5 representing lower aerosol loading in the boundary layer with weakly absorbing properties. Under such observed conditions, the uncertainties in both kinds of measurements are prone to be larger due to lower absorption signal relative to the instrumental noise and errors in algorithmic assumptions, such as surface albedo, that could further amplify the overall uncertainty in the retrievals. Despite these inherent uncertainties, an agreement within the difference of ±0.03 for about or more than half of the collocated retrievals is encouraging. A more detailed description of the different sources of uncertainty is presented in the next section.

Figure 3 shows the scatterplots of OMI-SKYNET SSA for remaining sites located in South Korea, China, Thailand, India, and Italy. For the site *Seoul* in South Korea, OMI tends to overestimate SSA for a number of matchups assigned with the urban/industrial aerosol type and for a few with the carbonaceous/smoke aerosol type such that about 42% of total matchups are falling within the difference of 0.03. For the *Dunhuang* site located in the desert area of China, a majority of collocated data points were identified as dust aerosol type providing an overall better agreement with 50% and 68% matchups bounded within ±0.03 and ±0.05 differences, respectively. The *Phimai* site in Thailand is known to be influenced by the springtime biomass burning activities, where OMI and SKYNET SSAs are found to agree relatively best among all 25 sites providing 71% and 91% of the matchups restricted within ±0.03 and ±0.05 limits,

https://doi.org/10.5194/amt-2019-174
Preprint. Discussion started: 25 June 2019


Atmospheric Measurement Techniques Discussions

respectively. The agreement between the two sensors was robust for the carbonaceous/smoke aerosol type followed by the urban/industrial aerosols. Over the megacity of New Delhi in the Indo-Gangetic Plain in India, which is seasonally influenced by the smoke and desert dust aerosols in addition to the local source of urban pollution, the OMI-SKYNET matchups are found to agree within ±0.03 and ±0.05 for 52% and 83% of the evaluated data points respectively. Over the *Pune* station located near the western boundary of India and the *Bologna* site in Italy, OMI retrieves higher SSA compared to that of SKYNET yielding 39% and 64%, and 25% and 50% matchups, respectively, within the two uncertainty limits. Table 1 lists the statistical measures of the OMI-SKYNET SSA comparison for all 25 sites.

3.2 Composites for Each Aerosol Type

Figure 4 displays the composite scatterplots of OMI versus SKYNET SSA derived by segregating the matchup points for each aerosol type from all 25 sites. The intention here is to evaluate the consistency between the two retrieval methods for each aerosol type separately and understand their relative differences. When identified as the carbonaceous/smoke aerosol type, the OMI-SKYNET matchups reveal relatively best comparison among the three major aerosol types with 61% and 84% data points falling within the absolute difference of 0.03 and 0.05, respectively, and providing the lowest (0.035) root-mean-square-difference between the two retrievals. The collocation procedure yields the lowest number of matchups (N=32) for desert dust aerosol type obtained mostly over the site of *Dunhuang* in China, resulting 50% and 72% of data points within the stated uncertainty limits. Among the three aerosol types, the collocated points assigned with the urban/industrial aerosol type (Figure 4 bottom-left) yield the maximum number of matchups (N=739) with the relatively weakest agreement (RMSD=0.052), where OMI tends to overestimate SSA for a significant number of instances resulting about 45% and 67% data points falling within the two limits of expected uncertainties. When more than one prescribed aerosol types are selected for OMI pixels around the SKYNET stations, the matchups between the two sensors resulted in 59% and 77% retrievals within the uncertainty limits with an RMSD of 0.041—a comparison slightly poorer than 'smoke-only' case, but better than 'dust-only' and 'urban/industrial-only' retrieval cases. Combined, all three distinct aerosol

https://doi.org/10.5194/amt-2019-174
Preprint. Discussion started: 25 June 2019

Atmospheric Measurement Techniques Discussions

types simultaneously yield the total number of matchups (N=1223) with an RMSD of 0.047 between OMI and SKYNET resulting 51% and 72% collocated data points falling within the absolute difference of 0.03 and 0.05 difference, respectively. When the restriction of AOD>0.3 is removed from the collocation procedure, allowing all matchups regardless of their respective AOD values, the total number of collocated data points was increased to more than twice (N=2691) albeit with a relatively weaker agreement yielding an RMSD of 0.06 and percent data points within the uncertainty limits reducing to 38% and 59%, respectively.

3.3 Diagnosis of OMAERUV Versus SKYNET

The SKYNET algorithm inverts the spectral sky radiances in conjunction with the direct AOD measurements to retrieve the real and imaginary parts of the refractive index and particle size distribution of cloud-free observations under all aerosol loading conditions. These inversion products are believed to be more stable and accurate at larger aerosol loadings and solar zenith angles due to stronger aerosol absorption signal and longer optical path (*Dubovik et al*., 2000). Similarly, a sensitivity analysis of the two-channel OMAERUV retrievals suggests that the retrieved AOD and SSA are susceptible to the small change in surface albedo at lower aerosol loading (*Jethva et al*., 2014). For instance, an absolute difference of 0.01 in the surface albedo leads to a change in AOD approximately by 0.1 and SSA by ~0.02.

Figure 5 (top) shows the absolute difference in collocated SSA between OMI and SKYNET as a function of concurrent SKYNET direct AOD (388 or 400 nm) measurements for all aerosol types. All OMI-SKYNET matchup data obtained from a total of 25 sites under all AOD conditions are included here. The data are shown in the box and whisker format, where the horizontal lines represent the median value of each bin of sample size 150, filled circle the mean value, and shaded vertical bars cover the 25 and 75 percentiles of the population in each bin. While for most bins the mean and median values of SSA difference were restricted to within ±0.03, OMI tends to overestimate SSA relative to that of SKYNET at lower AODs giving larger differences and spread in the data population. Similar patterns were observed when the difference in SSA was related to the OMI-retrieved AOD (Figure 5 middle). In both cases, the differences in SSA

https://doi.org/10.5194/amt-2019-174
Preprint. Discussion started: 25 June 2019

Atmospheric Measurement Techniques Discussions

334 minimize at larger AOD values (>0.5) suggesting a convergence in both retrievals. Figure 5
335 (bottom) shows a similar plot of SSA difference against the concurrent OMI UVAI. Notably, the
336 differences in SSA exhibit even a stronger relationship to UVAI than that in the AOD case (top
337 and middle). For UVAI lesser than zero, the differences in the retrieval are found to be beyond
338 the expected uncertainty in both inversions, at least in the mean sense. For the lower range of
339 UVAI, OMI algorithm mostly employs the urban/industrial model for the retrieval where all
340 aerosols are assumed to be confined within the boundary layer (<2 km) with a vertical profile
341 that follows an exponential distribution. On the other hand, the mean and median values of the
342 SSA difference for UVAI larger than 0.2 for all bins fall within the 0.03 uncertainty range. The
343 SSA differences approach to near-zero with a reduced spread at larger magnitudes. Notably,
344 both inversions are found to be in closer agreement for UVAI measurements>0.3.

345

346 # 4 SOURCES OF UNCERTAINTY

347 ## 4.1 UNCERTAINTIES IN THE GROUND-BASED SKYNET INVERSION PRODUCT

348 The SKYNET inversion algorithm assumes a wavelength-independent surface albedo of 0.1 at all
349 wavelengths across the UV to visible part of the spectrum. The diffuse light reflected from the
350 ground plays a second-order role in the measured sky radiances in most situations, however,
351 has a potential to affect the SSA inversion, e.g., overestimated (underestimated) surface albedo
352 can underestimate (overestimate) SSA (*Dubovik et al.*, 2000; *Khatri et al.*, 2012). Using
353 simultaneous inversion data from SKYNET and AERONET for four representative sites, *Khatri et*
354 *al.* (2016) have shown that the difference in the prescribed surface albedo between SKYNET
355 and AERONET results in a difference of ~0.04 in SSA at red (675 nm) and near-IR wavelengths
356 retrieved from the two collocated ground sensors. The difference in SSA can also reach as large
357 as ~0.08 when surface albedo differed by 0.3. The assumed surface albedo value of 0.1 at near-
358 UV (340 and 380 nm) and shorter visible wavelength (400 nm) seems to be unrealistic for the
359 vegetated and urban surfaces. The surface albedo database at 354 nm and 388 nm derived
360 from multiyear observations from OMI suggests that the vegetated surfaces and urban centers

https://doi.org/10.5194/amt-2019-174
Preprint. Discussion started: 25 June 2019

Atmospheric Measurement Techniques Discussions

361 are characterized with the lower values of surface albedo, i.e., ~0.02-0.03 and ~0.05,
362 respectively; for desert surfaces, the albedo could be as high as 0.08-0.10. Significant
363 differences in the assumed surface albedo values between OMI and SKYNET at shorter
364 wavelengths could be one of the responsible factors for discrepancies in SSA noted over several
365 sites, particularly at lower aerosol loading when the uncertainty in surface characterization can
366 amplify error in the SSA inversion.

367

368 To further investigate this effect, the difference in SSA between OMI and SKYNET as a function
369 of the simultaneous difference in surface albedo is analyzed and shown in Figure 6. The data
370 are presented in a standard box and whisker plot format. Figure 6 reveals a link between
371 differences in SSA and surface albedo, where increasing differences in SSA (OMI>SKYNET) are
372 associated with significant negative biases in surface albedo between OMI and SKYNET. In other
373 words, large overestimation in SKYNET surface albedo causes underestimation of retrieved SSA,
374 which is consistent with the findings of *Dubovik et al*. (2000) and *Khatri et al*. (2012, 2016),
375 thereby resulting in a substantial positive difference in SSA between OMI and SKYNET. Recently,
376 *Mok et al.* (2018) have shown that the use of AERONET surface albedo dataset at 440 nm in the
377 SKYNET algorithm for the S. Korea region produces SSA values larger by ~0.01 at near-UV
378 wavelengths. Notably, differences in SSA tend to be lower when the differences in surface
379 albedo are also minimal, such that the mean and median values of those bins remain within the
380 expected uncertainties of ±0. 03 in both retrievals. This result, along with the previous findings
381 cited above, convincingly points out that the SSA inversion from ground-based sensors,
382 especially at lower aerosol loadings, is likely susceptible to the prescribed surface albedo. The
383 assumption of a fixed value of spectral surface albedo of 0.1 in the SKYNET algorithm appears to
384 be inappropriate calling for a revision using more accurate datasets of spectral reflectance or
385 albedo such as from MODIS and OMI.

386

387 SKYNET inversion algorithm (Skyrad.pack Version 4.2 and version 5) assumes aerosols of
388 spherical shape regardless of the actual aerosol type observed in the scene. Following a

https://doi.org/10.5194/amt-2019-174
Preprint. Discussion started: 25 June 2019

Atmospheric Measurement Techniques Discussions

389 detailed analysis of the effect of non-sphericity of the particles on the difference between the
390 retrievals carried out assuming spherical and spheroidal size distribution, *Khatri et al*., (2016)
391 concluded that the assumed shape of particles has a non-significant impact on the retrieved
392 SSA. Their study revealed SSA difference of ±0.01 for measurements having a maximum
393 scattering angle <120° and difference of up to ±0.02 at scattering angle >120°, where the
394 difference in the phase function is significant between spherical and spheroidal size
395 distributions (*Torres et al*., 2018). The OMI-SKYNET collocation procedure, as shown in Figure 4,
396 yields relatively fewer matchups that are identified as dust aerosol type according to the
397 OMAERUV aerosol type identification scheme. A majority of the collocated data points were
398 derived over the desert site of *Dunhuang* in China showing a reasonable agreement in SSA
399 between OMI and SKYNET for dust aerosols further supporting the findings of *Khatri et al*.
400 (2016) that the SSA retrievals are not significantly impacted by the assumption of the shape of
401 particles, i.e., spherical or spheroidal.

402

403 Apart from the algorithmic assumptions, the calibration constant used for sky radiances
404 measured by SKYNET instruments can be a potential source of errors in the inversion. *Khatri et*
405 *al*. (2016) suggests that the calibration constant for sky radiances determined from the disk
406 scan method using solar disk scan area of 1° × 1° (*Boi et al*., (1999) may be underestimated
407 resulting in overestimated sky radiance and thus relatively higher SSA. Some of the larger
408 differences between in SSA between OMI and SKYNET, where OMI underestimates SSA relative
409 to the SKYNET, can be attributed to the imperfect calibration applied to the SKYNET sensors.

410 ### 4.2 Possible Sources of Uncertainties in OMAERUV Retrievals

411 Like other satellite-based remote sensing algorithms, OMAERUV also relies on assumptions
412 about the atmospheric and surface properties for the retrieval of aerosol properties. The single
413 largest known source of error in the OMI retrievals is the subpixel cloud contamination within
414 the OMI footprint. Given the footprint of size 13 × 24 km^2 for near-nadir pixels which intercept
415 an area of about 338 km^2 on the ground, the presence of subpixel clouds may not be avoided
416 entirely. Currently, the algorithm assigns quality flags to each pixel which carries information on

https://doi.org/10.5194/amt-2019-174
Preprint. Discussion started: 25 June 2019


Atmospheric Measurement Techniques Discussions

417 the quality of the retrieval depending upon the observed conditions (*Torres et al*., 2013).
418 Aerosol retrieval with the quality flag '0' are considered to be the best in accuracy as this
419 category of flag scheme largely avoids cloud-contaminated pixels by choosing the appropriate
420 thresholds in reflectivity and UVAI measurements.

421

422 Over the desert regions, e.g., the *Dunhuang* SKYNET site in China, the frequency of occurrence
423 of clouds is expected to be minimal. Therefore, it is less likely that the SSA retrievals over these
424 sites are affected by cloud contamination. A reasonable agreement between the two retrievals
425 (Figure 3) supports this assumption. The quality flag scheme, however, cannot entirely rule out
426 the presence of small levels of subpixel cloud contamination or the presence of thin cirrus in
427 the OMI footprint, which can cause overestimation in the retrieval of SSA, such as noted over
428 the SKYNET sites in *Kasuga*, *Etchujima*, *Seoul*, *Bologna*, and *Pune*.

429

430 Another possible source of uncertainty can be the assumption of the aerosol layer height. The
431 climatology of aerosol layer height derived from CALIOP measurements adequately describes
432 the observed mean layer of carbonaceous and desert dust aerosols (*Torres et al*., 2013). It is
433 particularly robust over the arid and semiarid areas where large numbers of cloud-free
434 observations were used in the calculation. However, note that the temporal and spatial
435 coverage of CALIOP is limited to 16-day repeat cycle over the same location. Variations in the
436 aerosol layer height not observed by CALIOP, therefore, will be missed out in the derived
437 climatology and thus can be a source of uncertainty. Sensitivity analysis of the OMAERUV
438 retrievals suggests that an overestimation (underestimation) in the aerosol layer height results
439 in an overestimated (underestimated) SSA. This is because an increase (decrease) in the aerosol
440 layer height from the actual one enhances (reduces) absorption signal in the radiance
441 measurements in near-UV, which the OMAERUV algorithm compensates by retrieving higher
442 AOD and SSA to match with the observations.

443

https://doi.org/10.5194/amt-2019-174
Preprint. Discussion started: 25 June 2019

Atmospheric Measurement Techniques Discussions

444 The third source of uncertainty that can affect SSA retrieval is the accuracy of the prescribed
445 surface albedo. For the surface characterization, the OMAERUV algorithm use a near-UV
446 surface albedo database derived using the multiyear OMI reflectivity observations. The method
447 adopts a minimum reflectivity approach, ensuring minimal or no contamination from the
448 atmosphere, i.e., aerosols and clouds, in the measurements. Afterward, the minimum
449 reflectivity dataset derived from the OMI observations was adjusted in the temporal domain to
450 the seasonality of surface albedo retrieved in the visible wavelengths from MODIS. The dataset
451 contains surface albedo values at 354 and 388 nm at a grid resolution of 0.25° × 0.25°.
452 Compared to the previous OMAERUV dataset using TOMS-based surface albedo product at 1°
453 grid resolution, the new OMI-based dataset is expected to be more accurate to within 0.005 to
454 0.01 owing to its higher spatial resolution and the fact that it is contemporary to the OMI
455 operation. A sensitivity study of the OMAERUV retrievals to the change in surface albedo
456 described in *Jethva et al*. (2014) suggests that an increase in surface albedo by 0.01 in the near-
457 UV region over desert areas results in a decrease in the magnitude of retrieved SSA by ~ -0.02.
458 The effect of uncertain surface albedo can be more pronounced at lower aerosol loading,
459 where the reduced signal from the atmosphere makes OMAERUV retrieval more susceptible to
460 the uncertainty in surface albedo.

461

462 The assumed aerosol microphysical and optical properties could be additional sources of
463 uncertainty. The particle size distributions assumed in the OMAERUV models are adopted from
464 long-term AERONET inversion statistics (*Dubovik et al*., 2002), representing areas influenced by
465 smoke, dust, and urban/industrial aerosols, and therefore are considered realistic
466 representations of the total atmospheric column. The carbonaceous smoke aerosols are
467 assumed to be spherical in shape with a bimodal log-normal size distribution and characterized
468 with a steep absorption gradient, such that the Absorption Angstrom Exponent (AAE) in the
469 near-UV lies in the range 2.5-3.0, to adequately represent the organics in the biomass burning
470 smoke particles (*Kirchstetter et al*., 2004; *Jethva and Torres*, 2011). The desert dust aerosol
471 model follows bimodal log-normal size distribution with particles comprised of randomly
472 oriented spheroids with an axis ratio (shape factor) distribution adopted from *Dubovik et al*.

https://doi.org/10.5194/amt-2019-174
Preprint. Discussion started: 25 June 2019

Atmospheric Measurement Techniques Discussions

(2006). The spectral dependence of the refractive index in the near-UV assumed in the dust aerosol model is generally consistent with the in-situ laboratory measurements (*Wagner et al.*, 2012). For instance, retrieval of AOD and SSA for carbonaceous aerosols using the smoke model with AAE of 1.90 (10% relative spectral dependence in the imaginary index between 354 and 388 nm) and 1.0 (no spectral dependence in the imaginary index), instead of the standard AAE assumption of 2.7, results in a decrease in SSA up to -0.07, respectively, suggesting a marked sensitivity of the SSA retrieval to the significant changes in the spectral aerosol absorption. Due to the shortage of ground-based characterization of absorption in the near-UV part of the spectrum, the regional representation of the spectral absorption properties in the OMAERUV models is limited. Therefore, spatial and temporal variations in the actual aerosol spectral properties can be a potential source of error in the SSA retrieval.

5 SUMMARY AND CONCLUSION

We presented a comparative analysis of the aerosol SSA retrieved from the OMI's two-channel aerosol algorithm (OMAERUV) against an independent ground-based inversion made by the SKYNET Sun photometers over selected 25 sites located mainly in Asia and Europe. This study follows our previous efforts of evaluating the OMI near-UV SSA product carried out using ground-based AERONET dataset (*Jethva et al.*, 2014). The capability of SKYNET sensors to measure the Sun and sky radiance at near-UV wavelengths (340-380-400 nm), and subsequently retrieve the aerosol optical properties, including SSA, at these wavelengths provide a unique opportunity to directly compare the two near-UV SSA products from ground and satellite. Ground-based inversion of SSA at the near-UV wavelengths eliminate the need to adjust and extrapolate satellite retrieval to the visible wavelengths such as the case with comparison against AERONET. Since the SSA inferred from two different platforms are essentially retrieved from two fundamentally different inversion algorithms, the present study does not stand as a "validation" exercise for either retrieval data sets. Instead, the purpose of this analysis was to check the consistency (or lack thereof) between the two retrieved

https://doi.org/10.5194/amt-2019-174
Preprint. Discussion started: 25 June 2019


Atmospheric Measurement Techniques Discussions

500 quantities of the same physical parameter regarding standard statistical comparison, i.e., RMSD
501 and % of matchups within the expected uncertainties.

502

503 Unlike AERONET Level 2 inversion product that reports spectral SSA when AOD (440 nm)
504 exceeds a value of 0.4, SKYNET Level 2 dataset delivers spectral SSA in the near-UV and visible
505 parts of the spectrum under all cloud-free observations for all AOD conditions. The collocation
506 procedure that matched temporal inversion data from SKYNET with spatial retrievals from OMI
507 gave resulted in a total of 2691 collocated data points for AOD>0.0 and 1223 when AOD>0.3
508 collected from 25 sites representing biomass burning region of Southeast Asia, desert in China,
509 and urban/industrial areas in Japan, India, and Europe. Combinedly for all 25 sites and under all
510 AOD conditions, we find 38% and 59% of the total SKYNET-OMI SSA agree within their
511 estimated uncertainty range of ±0.03 and ±0.05, respectively, with an overall root-mean-
512 square-difference of 0.06. When restricted with condition AOD>0.3 in both measurements, the
513 agreement of comparison improved to 51% and 72% with root-mean-square-difference of
514 0.047. When segregated by aerosol type, the agreement between the two sensors is found to
515 be robust for matchups identified as the carbonaceous aerosols over several sites in Japan,
516 *Seoul* in South Korea, *Phimai* in Thailand, and *New Delhi* in India, yielding 61% and 84% of data
517 points falling within the limits of ±0.03 and ±0.05 with an overall RMSD of 0.035. The
518 collocation procedure found few matchups for desert dust aerosol, mostly over *Dunhuang* site
519 in China, showing a reasonable comparison with 50% and 68% data points within expected
520 uncertainty limits. Among the three major aerosol types, the urban/industrial type aerosols
521 provide the maximum number of matchup data points with a relatively poorer comparison,
522 where 45% and 67% data are found to be within the uncertainty limits.

523

524 The differences in SSA between OMI and SKYNET are found to be largest at lower aerosol
525 loading, where OMI retrieves significantly higher SSA compared to that of SKYNET. However,
526 the differences are minimized at larger AOD values (>0.5) suggesting a convergence in both
527 retrievals at moderate to large aerosol loading. Similarly, the differences in SSA exhibit a

https://doi.org/10.5194/amt-2019-174
Preprint. Discussion started: 25 June 2019

Atmospheric Measurement Techniques Discussions

528 stronger relationship to UVAI showing larger discrepancies beyond expected uncertainty limits
529 at lower UVAIs (<0), but nearing to zero with a reduced spread in matchups at larger
530 magnitudes of UVAI (>0.2-0.3).

531

532 Much of the inconsistency observed between OMI and SKYNET at lower aerosol loadings
533 indicate retrieval issues due to reduced signal-to-noise ratio and uncertain algorithmic
534 assumptions. For instance, the OMAERUV retrievals are more susceptible to the changes in
535 surface albedo at lower AODs, and to the spectral absorption at higher AODs (*Torres and Jethva*,
536 2011). On the other hand, the SKYNET inversion algorithm assumes a wavelength-independent
537 surface albedo of 0.1 across the UV to visible-near-IR wavelengths, which appears to be
538 unrealistic especially in the UV region where OMI surface albedo dataset shows much lower
539 values (<0.05) over land. Though the reflected light from surface plays a second-order role in
540 the ground-based retrievals, previous studies as well as shown in the present work (Figure 6),
541 uncertainty in surface albedo can cause non-negligible errors in SSA retrievals that likely exceed
542 the expected accuracy level of ±0.03.

543

544 Despite the inherent uncertainties associated with both satellite and ground inversion products,
545 a good level of agreement between the two independent techniques over SKYNET sites at
546 increasing aerosol loading is encouraging. We intend to extend the present analysis to other
547 SKYNET sites whose data are still not directly accessible in the public domain. Continuing the
548 evaluation of inversion products, both from satellite and ground, is an important exercise to
549 track the changes and improvements in the algorithms and resulting data products, and to
550 establish the consistency (or lack thereof) that can help to diagnose further and improve the
551 accuracy of retrievals.

552

https://doi.org/10.5194/amt-2019-174
Preprint. Discussion started: 25 June 2019

Atmospheric Measurement Techniques Discussions

ACKNOWLEDGMENTS

We thank the Center for Environmental Remote Sensing (CERes), Chiba University, Japan (http://atmos3.cr.chiba-u.jp/skynet/data.html), for the online availability of the SKYNET dataset for several sites in Japan, South Korea, China, India, Italy, and Germany. Acknowledgments are also due to the principal investigators and their staff for establishing and maintaining respective SKYNET sites, whose data are used in the present work. We acknowledge the support of NASA GES-DISC, the NASA Earth Science data center, for the online availability of the OMI aerosol product assessed in this analysis.

https://doi.org/10.5194/amt-2019-174
Preprint. Discussion started: 25 June 2019

Atmospheric Measurement Techniques Discussions

AUTHORS' CONTRIBUTIONS

Dr. Jethva, the leading author, conceptualized the study and wrote the paper. He conducted comparative data analysis of OMI- and SKYNET-retrieved single-scattering albedo products presented in the paper. Dr. Torres (2nd author) brought his expertise in interpreting the results and helped improving the manuscript writeup.

Additional Information

The author(s) declare no competing interests, financial or non-financial.

https://doi.org/10.5194/amt-2019-174
Preprint. Discussion started: 25 June 2019

Atmospheric Measurement Techniques Discussions

REFERENCES

Ahn, C., O. Torres, and P. K. Bhartia: Comparison of Ozone Monitoring Instrument UVAerosol Products with Aqua/Moderate Resolution Imaging Spectroradiometer and Multiangle Imaging Spectroradiometer observations in 2006, J. Geophys. Res., 113, D16S27, doi:10.1029/2007JD008832, 2008.

Ahn, C., O. Torres, and H. Jethva: Assessment of OMI near-UV aerosol optical depth over land, J. Geophys. Res. Atmos., 119, doi:10.1002/ 2013JD020188, 2014.

Boi, P., G. Tonna, G. Dalu, T. Nakajima, B. Olivieri, A. Pompei, M. Campanelli, and R. Rao: Calibration and data elaboration procedure for sky irradiance measurements, Appl. Opt., 38, 896-907, 1999.d

Campanelli, M., T. Nakajima, B. Olivieri: Determination of the solar calibration constant for a sun-sky radiometer, Applied Optics, 43(3), 2004.

Campanelli, M., G. Gobbi, C. Tomasi, and T. Nakajima: Intercomparison between aerosol characteristics retrieved simultaneously with a Cimel and Prede Sun-sky radiometers in Rome (TorVergata AERONET site), Opt. Pura Apl., 37, 3159–3164, 2004a.

Campanelli, M., V. Estelles, C. Tomasi, T. Nakajima, V. Malvestuto and J. A. Martinez-Lozan: Application of the SKYRAD improved Langley plot method for the in situ calibration of CIMEL sun-sky photometers, Applied Optics, 46(14), 2007.

Campanelli, M., A. M. Iannarelli , S. Kazadzis, N. Kouremeti, S. Vergari, V. Estelles, H. Diemoz, A. di Sarra, A. Cede: The QUATRAM Campaign: QUAlity and TRaceabiliy of Atmospheric aerosol Measurements, The 2018 WMO/CIMO Technical Conference on Meteorological and Environmental Instruments and Methods of Observation (CIMO TECO-2018) “Towards fit-for-purpose environmental measurements”, 2018.

Che, H., G. Shi, A. Uchiyama, A. Yamazaki, H. Chen, P. Goloub, and X. Zhang: Intercomparison between aerosol optical properties by a PREDE skyradiometer and CIMEL sunphotometer over Beijing, China, Atmos. Chem. Phys., 8, 3199-3214, doi:10.5194/acp-8-3199-2008, 2008.

Dubovik, O., A. Smirnov, B. N. Holben, M. D. King, Y. J. Kaufman, T. F. Eck, and I. Slutsker, Accuracy assessments of aerosol optical properties retrieved from Aerosol Robotic Network

https://doi.org/10.5194/amt-2019-174
Preprint. Discussion started: 25 June 2019

Atmospheric Measurement Techniques Discussions

606 (AERONET) Sun and sky radiance measurements, J. Geophys. Res., 105(D8), 9791-9806,
607 doi:10.1029/2000JD900040, 2000.
608
609 Dubovik, O., B. N. Holben, T. F. Eck, A. Smirnov, Y. J. Kaufman, M. D. King, D. Tanre, and I.
610 Slutsker: Variability of absorption and optical properties of key aerosol types observed in
611 worldwide locations, J. Atmos. Sci., 59, 590–608, 2002.
612
613 Dubovik, O., Sinyuk, A., Lapyonok, T., Holben, B. N., Mishcenko, M., Yang, P., Eck, T. F., Volten,
614 H., Munoz, O., Vehelmann, B., van der Zande, W. J., Leon, J. F., Sorokin, M., and Slutsker, I.:
615 Application of spheroid models to account for aerosol particle nonsphericity in remote sensing
616 of desert dust, J. Geophys. Res., 111, D11208, https://doi.org/10.1029/2005JD006619, 2006.
617
618 Estellés, V., Campanelli, M., Smyth, T. J., Utrillas, M. P., and Martínez-Lozano, J. A.: Evaluation of
619 the new ESR network software for the retrieval of direct sun products from CIMEL CE318 and
620 PREDE POM01 sun-sky radiometers, Atmos. Chem. Phys., 12, 11619-11630,
621 https://doi.org/10.5194/acp-12-11619-2012, 2012a.
622
623 Estellés, V., Campanelli, M., Utrillas, M. P., Expósito, F., and Martínez-Lozano, J. A.: Comparison
624 of AERONET and SKYRAD4.2 inversion products retrieved from a Cimel CE318 sunphotometer,
625 Atmos. Meas. Tech., 5, 569-579, https://doi.org/10.5194/amt-5-569-2012, 2012b.
626
627 Estelles, V., N. Kouremeti, M. Campanelli, J. Grobner, J.A. Mari nez-Lozano, S. Kazadzis:
628 Preliminary aerosol optical depth comparison between ESR/SKYNET, AERONET and GAW
629 international networks. International SKYNET workshop, Rome (Italy), 2016.
630
631 Khatri, P., and T. Takamura: An algorithm to screen cloud affected data for sky radiometer data
632 analysis, J. Meteor. Soc. Japan, 87, 189-204, 2009.
633
634 Khatri, P., T. Takamura, A. Yamazaki, and Y. Kondo: Reterival of key aerosol optical parameters
635 for spectral direct and diffuse irradiances measured by a horizontal surface detector, J. Atmos.
636 Oceanic Technol., 29, 683–696, 2012.
637
638 Khatri, P., T. Takamura, T. Nakajima, V. Estellés, H. Irie, H. Kuze, M. Campanelli, A. Sinyuk, S.-M.
639 Lee, B. J. Sohn, G. Pandithurai, S.-W. Kim, S. C. Yoon, J. A. Martinez-Lozano, M. Hashimoto, P. C.
640 S. Devara, and N. Manago: Factors for inconsistent aerosol single scattering albedo between
641 SKYNET and AERONET, J. Geophys. Res. Atmos., 121, 1859-1877, doi:10.1002/2015JD023976,
642 2016.
643

https://doi.org/10.5194/amt-2019-174
Preprint. Discussion started: 25 June 2019

Atmospheric Measurement Techniques Discussions

644 Kirchstetter, T. W., T. Novakov, and P. V. Hobbs: Evidence that the spectral dependence of light
645 absorption by aerosols is affected by organic carbon, J. Geophys. Res., 109, D21208,
646 doi:10.1029/2004JD004999, 2004.
647
648 Hansen, J., M. Sato, and R. Ruedy: Radiative forcing and climate response, J. Geophys. 795 Res.,
649 102(D6), 6831-6864, doi:10.1029/96JD03436, 1997.
650
651
652 Hashimoto, M., Nakajima, T., Dubovik, O., Campanelli, M., Che, H., Khatri, P., Takamura, T., and
653 Pandithurai, G.: Development of a new data-processing method for SKYNET sky radiometer
654 observations, Atmos. Meas. Tech., 5, 2723-2737, https://doi.org/10.5194/amt-5-2723-2012,
655 2012.
656
657 IPCC, 2013: Climate Change 2013: The Physical Science Basis. Contribution of Working Group I
658 to the Fifth Assessment Report of the Intergovernmental Panel on Climate Change (Stocker, T.F.,
659 D. Qin, G.-K. Plattner, M. Tignor, S.K. Allen, J. Boschung, A. Nauels, Y. Xia, V. Bex and P.M.
660 Midgley (eds.)). Cambridge University Press, Cambridge, United Kingdom and New York, NY,
661 USA, 1535 pp, doi:10.1017/CBO9781107415324.
662
663 Jethva, H., and O. Torres: Satellite-based evidence of wavelength-dependent aerosol absorption
664 in biomass burning smoke inferred from Ozone Monitoring Instrument, Atmos. Chem. Phys., 11,
665 10,541–10,551, doi:10.5194/acp-11-10541-2011, 2011.
666
667 Jethva, H., O. Torres, and C. Ahn: Global assessment of OMI aerosol single-scattering albedo
668 using ground-based AERONET inversion, J. Geophys. Res. Atmos., 119,
669 doi:10.1002/2014JD021672, 2014.
670
671 Mok, J., Krotkov, N. A., Torres, O., Jethva, H., Li, Z., Kim, J., Koo, J.-H., Go, S., Irie, H., Labow, G.,
672 Eck, T. F., Holben, B. N., Herman, J., Loughman, R. P., Spinei, E., Lee, S. S., Khatri, P., and
673 Campanelli, M.: Comparisons of spectral aerosol single scattering albedo in Seoul, South Korea,
674 Atmos. Meas. Tech., 11, 2295-2311, https://doi.org/10.5194/amt-11-2295-2018, 2018.
675
676 Nakajima, T., G. Tonna, R. Rao, P. Boi, Y. Kaufman, and B. Holben: Use of sky brightness
677 measurements from ground for remote sensing of particulate polydispersions, Appl. Opt., 35,
678 15, 2672-2686, 1996.
679

https://doi.org/10.5194/amt-2019-174
Preprint. Discussion started: 25 June 2019

Atmospheric Measurement Techniques Discussions

680 Schenkeveld, V. M. E., Jaross, G., Marchenko, S., Haffner, D., Kleipool, Q. L., Rozemeijer, N. C.,
681 Veefkind, J. P., and Levelt, P. F.: In-flight performance of the Ozone Monitoring Instrument,
682 Atmos. Meas. Tech., 10, 1957–1986, https://doi.org/10.5194/amt-10-1957-2017, 2017.
683
684 Torres, O., P. K. Bhartia, J. R. Herman, Z. Ahmad, and J. Gleason: Derivation of aerosol
685 properties from satellite measurements of backscattered ultraviolet radiation: Theoretical basis,
686 J. Geophys. Res., 103(D14), 17,099–17,110, doi:10.1029/98JD00900, 1998.

687 Torres, O., P. K. Bhartia, A. Sinyuk, E. J. Welton, and B. Holben:Total Ozone Mapping
688 Spectrometer measurements of aerosol absorption from space: Comparison to SAFARI 2000
689 ground-based observations, J. Geophys. Res., 110, D10S18, doi:10.1029/2004JD004611, 2005
690
691 Torres, O., A. Tanskanen, B. Veihelmann, C. Ahn, R. Braak, P. K. Bhartia, P. Veefkind, and P.
692 Levelt: Aerosols and surface UV products from Ozone Monitoring Instrument observations: An
693 overview, J. Geophys. Res., 112, D24S47, doi:10.1029/2007JD008809, 2007.

694 Torres, O., C. Ahn, and Z. Chen: Improvements to the OMI near-UV aerosol algorithm using A-
695 train CALIOP and AIRS observations, Atmos. Meas. Tech., 6, 3257–3270, doi:10.5194/amt-6-
696 3257-2013, 2013.

697 Torres, O., Bhartia, P. K., Jethva, H., and Ahn, C.: Impact of the ozone monitoring instrument
698 row anomaly on the long-term record of aerosol products, Atmos. Meas. Tech., 11, 2701-2715,
699 https://doi.org/10.5194/amt-11-2701-2018, 2018.

700 Wagner, R., T. Ajtai, K. Kandler, K. Lieke, C. Linke, T. Müller, M. Schnaiter, and M. Vragel:
701 Complex refractive indices of Saharan dust samples at visible and near UV wavelengths: A
702 laboratory study, Atmos. Chem. Phys., 12, 2491–2512, doi:10.5194/acp-12-2491-2012, 2012.

703

https://doi.org/10.5194/amt-2019-174
Preprint. Discussion started: 25 June 2019

Atmospheric Measurement Techniques Discussions

TABLES

Table 1 A list of SKYNET sites and corresponding dataset used in the present analysis. Sensor type "POM02" consists of a total of seven wavelength filters, including near-UV bands, i.e., 340, 380, 400, 500, 675, 870, and 1020 nm, whereas "POM01" sensors have a total of five wavelength filters, i.e., 400, 500, 675, 870, and 1020 nm. The rightmost four columns enlist the statistical measures of OMI-SKYNET single-scattering albedo matchups.

Abbreviations: N: number of satellite-ground matchups, RMSD: root-mean-square-difference between OMI and SKYNET, Q_0.03 and Q_0.05: percent matchups within an absolute difference of 0.03 and 0.05.

SKYNET Station Name	Longitude	Latitude	Country	Sensor Type	Data Period	N	RMSD	Q_0.03 (%)	Q_0.05 (%)
Chiba University	140.104°E	35.625°N	Japan	POM02	2005-2017	132	0.039	58	81
Cape Hedo	128.248E	26.867N	Japan	POM02	2005-2017	47	0.044	47	72
Fukue	128.682E	32.752N	Japan	POM02	2008-2017	71	0.041	59	76
Miyako	125.327E	24.737N	Japan	POM02	2004-2017	31	0.059	23	58
Sendai	140.84E	38.26N	Japan	POM01	2009-2017	34	0.052	50	74
Kasuga	130.475E	33.524N	Japan	POM02	2004-2017	159	0.057	40	61
Saga	130.283E	33.233N	Japan	POM02	2011-2017	66	0.044	52	71
Minamitorishima	153.97E	24.3N	Japan	POM02	2006-2009	-	-	-	-
Moshiri	142.260E	44.366N	Japan	POM02	2009-2011	2	0.018	100	100
Fuji Hokuroku	138.750E	35.433N	Japan	POM02	2009-2017	9	0.051	56	67
Tsukuba	140.096E	36.114N	Japan	POM02	2014-2017	5	0.027	80	100
Takayama	137.423E	36.145N	Japan	POM02	2014-2017	3	0.022	67	100
Etchujima	139.796E	35.664N	Japan	POM01	2004-2010	100	0.052	45	66
Seoul	126.95E	37.46N	Republic of South Korea	POM01	2005-2015	182	0.050	42	66
Yonsei	126.980E	37.570N	Republic of South Korea	POM02	2016	5	0.035	40	80
Dunhuang	90.799E	40.146N	China	POM01	1999-2007	40	0.048	50	68
Phimai	102.564E	15.184N	Thailand	POM02	2005-2017	139	0.031	71	91
Bangkok	100.605E	13.667N	Thailand	POM02	2009-2017	15	0.064	47	60
Mandalgovi	106.264E	45.743N	Mongolia	POM01	1998-2009	4	0.087	0	0
Ulan Bator	106.921E	47.923N	Mongolia	POM01	2013-2017	2	0.026	100	100
New Delhi	77.174E	28.629N	India	POM01	2006-2007	63	0.038	52	83
Pune	73.805E	18.537N	India	POM01	2004-2009	94	0.050	39	64
Bologna	11.34E	44.52N	Italy	POM02	2014-2017	114	0.065	25	50
Valencia	0.420E	39.507N	Spain	POM01	2014-2017	4	0.052	25	25
Bremen	8.854E	3.108N	Germany	POM02	2009	-	-	-	-

https://doi.org/10.5194/amt-2019-174
Preprint. Discussion started: 25 June 2019

Atmospheric Measurement Techniques Discussions

FIGURES

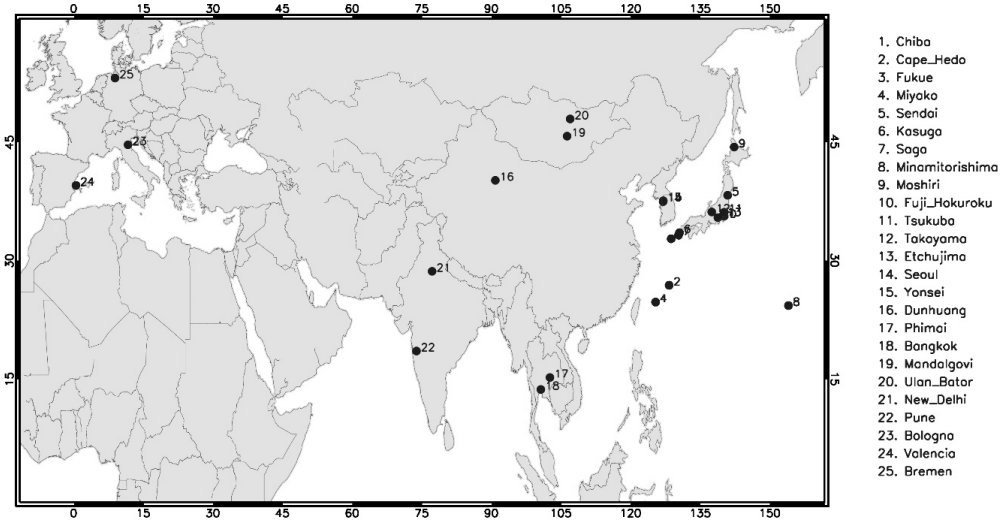

Figure 1 Geographical placement of ground-based SKYNET sensors over sites in Asia and Europe The SKYNET dataset for these sites are freely accessible from the Center for Environmental Remote Sensing (CERes), Chiba University, Japan (http://atmos3.cr.chiba-u.jp/skynet/data.html).

https://doi.org/10.5194/amt-2019-174
Preprint. Discussion started: 25 June 2019

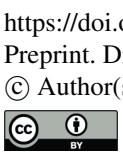

Atmospheric Measurement Techniques Discussions

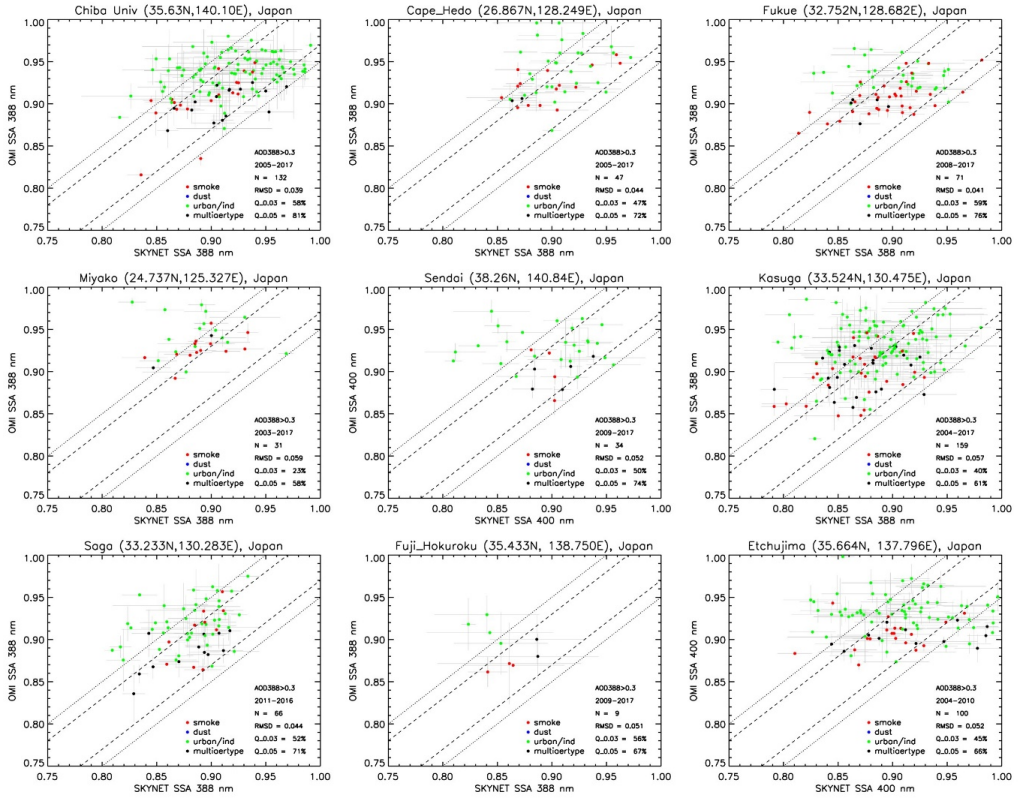

719

720 **Figure 2** OMAERUV versus SKYNET single-scattering albedo comparison for different sites in
721 Japan. Legends with different colors represent the aerosol type selected by the OMAERUV
722 algorithm for the co-located matchups (N). RMSD is the root-mean-square difference between
723 the two retrievals; Q_0.03 and Q_0.05 are the percents of total matchups (N) that fall within
724 the absolute difference of 0.03 and 0.05, respectively. OMI-SKYNET matchups with AOD>0.3
725 (388 or 400 nm) in both measurements are used for comparison.

726

727

https://doi.org/10.5194/amt-2019-174
Preprint. Discussion started: 25 June 2019

Atmospheric Measurement Techniques Discussions

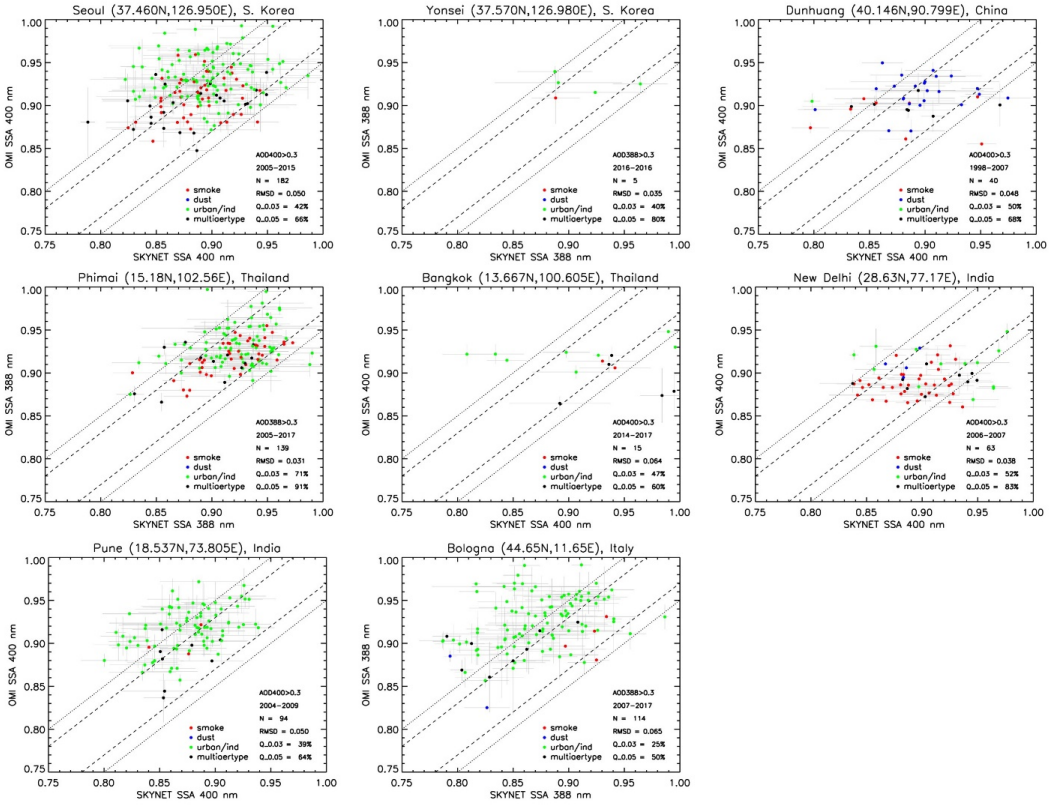

728

729 **Figure 3** Same as in Figure 2 but for SKYNET sites in South Korea, China, Thailand, India, and

730 Italy.

https://doi.org/10.5194/amt-2019-174
Preprint. Discussion started: 25 June 2019

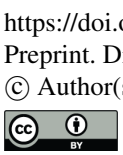

Atmospheric Measurement Techniques Discussions

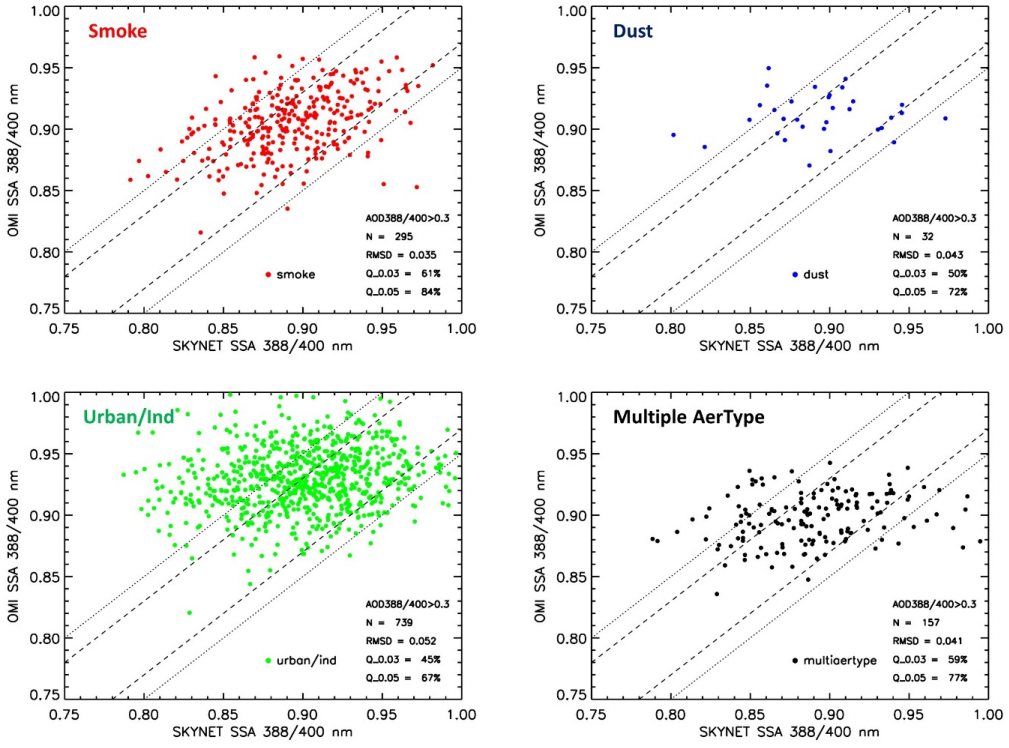

731

732 **Figure 4** Composite scatterplots of OMAERUV versus SKYNET single-scattering albedo (388 or
733 400 nm) for the three distinct aerosol types, i.e., smoke, dust, and urban/industrial, as
734 identified by the OMAERUV algorithm. OMI-SKYNET matchups with AOD>0.3 (388 or 400 nm) in
735 both measurements are used for the comparison.

736

https://doi.org/10.5194/amt-2019-174
Preprint. Discussion started: 25 June 2019

Atmospheric Measurement Techniques Discussions

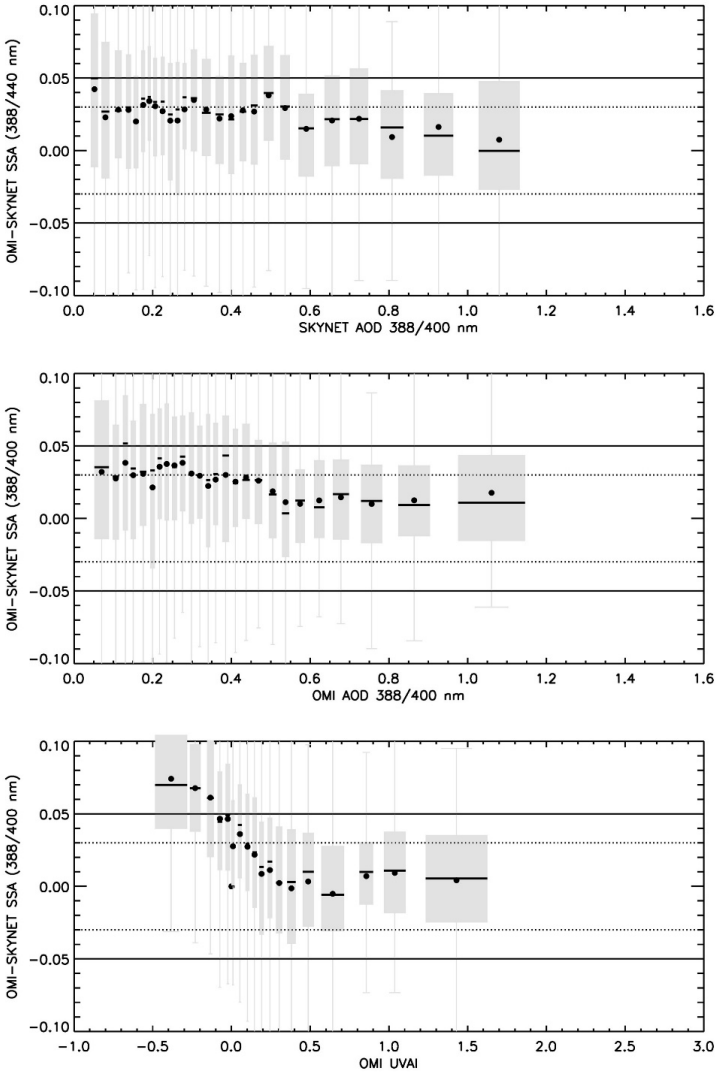

737

738 **Figure 5** Difference in single-scattering albedo between OMI and SKYNET as a function of the
739 coincident SKYNET-measured (top panel) and OMI-retrieved (middle panel) aerosol optical
740 depth and OMI-measured UVAI (bottom panel). Filled circles in black are the mean of difference
741 for each AOD and UVAI bin with an equal sample size of 150 matchups; horizontal lines
742 represent median of the bin samples; shaded area in gray encompasses data within 25 (lower)
743 to 75 (higher) percentile range, whereas vertical lines in gray represent 1.5 times inter-quartile
744 range (25 to 75 percentile). The dotted and solid horizontal lines are the uncertainty range of
745 ±0.03 and ±0.05 respectively.

https://doi.org/10.5194/amt-2019-174
Preprint. Discussion started: 25 June 2019

Atmospheric Measurement Techniques Discussions

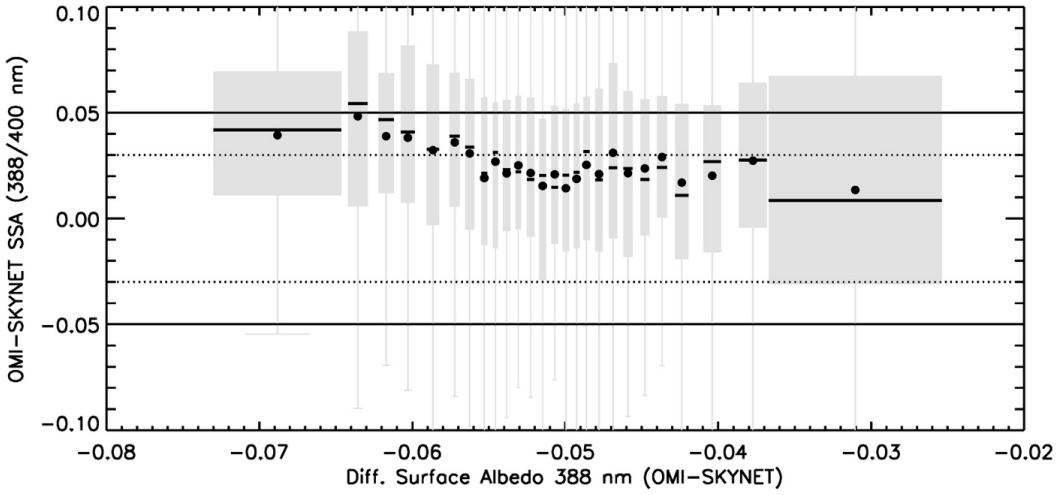

746
747 **Figure 6** Same as in Figure 5 but the difference in SSA between OMI and SKYNET is related to
748 the difference in surface albedo assumed by the two algorithms.